JACS
JOURNAL OF THE AMERICAN CHEMICAL SOCIETY
Article
pubs.acs.org/JACS

Reversible Unfolding and Folding of the Metalloprotein Ferredoxin Revealed by Single-Molecule Atomic Force Microscopy

Hai Lei,[†,‡] Yabin Guo,[‡] Xiaodong Hu,[†] Chunguang Hu,[†] Xiaotang Hu,[†] and Hongbin Li*[,†,‡]

[†]State Key Laboratory of Precision Measurements Technology and Instruments, School of Precision Instrument and Optoelectronics Engineering, Tianjin University, Tianjin 300072, People's Republic of China

[‡]Department of Chemistry, University of British Columbia, Vancouver, British Columbia V6T 1Z1, Canada

Supporting Information

ABSTRACT: Plant type [2Fe-2S] ferredoxins function primarily as electron transfer proteins in photosynthesis. Studying the unfolding−folding of ferredoxins in vitro is challenging, because the unfolding of ferredoxin is often irreversible due to the loss or disintegration of the iron−sulfur cluster. Additionally, the in vivo folding of holo-ferredoxin requires ferredoxin biogenesis proteins. Here, we employed atomic force microscopy-based single-molecule force microscopy and protein engineering techniques to directly study the mechanical unfolding and refolding of a plant type [2Fe-2S] ferredoxin from cyanobacteria *Anabaena*. Our results indicate that upon stretching, ferredoxin unfolds in a three-state mechanism. The first step is the unfolding of the protein sequence that is outside and not sequestered by the [2Fe-2S] center, and the second one relates to the force-induced rupture of the [2Fe-2S] metal center and subsequent unraveling of the protein structure shielded by the [2Fe-2S] center. During repeated stretching and relaxation of a single polyprotein, we observed that the completely unfolded ferredoxin can refold to its native holo-form with a fully reconstituted [2Fe-2S] center. These results demonstrate that the unfolding−refolding of individual ferredoxin is reversible at the single-molecule level, enabling new avenues of studying both folding−unfolding mechanisms, as well as the reactivity of the metal center of metalloproteins in vitro.

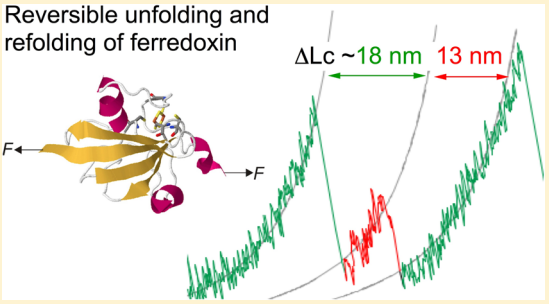

INTRODUCTION

Metalloproteins are ubiquitously present and play vital roles in biology.[1−4] Metal centers within metalloproteins often serve as enzymatic active centers for catalyzing chemical reactions, and thus significantly broaden the functionality of proteins. Metal centers within metalloproteins can also serve as important structural sites to both facilitate protein folding and enhance protein stability.[5,6] The loss of these metal centers will inactivate these functions, and may cause protein misfolding, which can have significant biological consequences.[7−9] Understanding the role that metal centers play in the folding/unfolding of metalloproteins, as well as the relationship between metal centers and protein stability, is thus of critical importance. The unfolding/folding mechanisms of some simple Cu- and Fe-containing metalloproteins have been investigated using classical ensemble biophysical techniques (such as far-UV circular dichroism, electron paramagnetic resonance spectroscopy, and Raman spectroscopy). These studies revealed that the binding of metal ions to the unfolded polypeptide chain could provide a nucleation site to facilitate metalloproteins folding.[5,10] However, studying the folding and unfolding behavior of metalloproteins remains challenging because metalloproteins unfolding is often irreversible, possibly due to the loss or disintegration of the metal center or metal cluster. Developing new experimental tools to study the unfolding and folding mechanism of such metalloproteins thus remains an important and unsolved task.

Over the last two decades, atomic force microscopy (AFM)-based force spectroscopy has developed into a powerful and generally applicable methodology for studying unfolding and folding mechanisms of proteins, ranging from elastomeric proteins to membrane proteins, at the single-molecule level.[11−16] These studies have revealed unique and otherwise difficult to observe insights into protein folding and unfolding mechanisms. Recently, we demonstrated the utility of this powerful technique for studying metalloproteins using the simplest iron sulfur protein rubredoxin as a model system.[17−20] We observed that stretching rubredoxin along a well-defined direction caused it to unfold and its FeS_4 center to rupture. Our studies not only reveal the detailed mechanism behind the mechanical unfolding of rubredoxin (including the release of iron), but also provide direct experimental evidence for the iron-priming mechanism proposed for rubredoxin folding. Our studies thus pave the way for using single-molecule AFM as a novel experimental tool to investigate the folding−unfolding mechanisms of metalloproteins.[21−24] Here, we employed protein engineering and single-molecule AFM techniques to demonstrate the feasibility of investigating difficult to study

Received: November 1, 2016
Published: January 11, 2017

DOI: 10.1021/jacs.6b11371
J. Am. Chem. Soc. 2017, 139, 1538−1544

unfolding−folding mechanisms for a plant type [2Fe-2S] ferredoxin in vitro.[25]

Plant type [2Fe-2S] ferredoxins are a unique member of the ferredoxins family. They are found in plants, algae, and cyanobacteria, and serve as electron transfer proteins within photosynthesis.[26] During its folding in vivo, holo-ferredoxins requires the assistance of iron sulfur biogenesis proteins.[27] Studying unfolding−folding mechanisms of ferredoxins in vitro is challenging, as unfolding tends to be irreversible. Thus, we employed single-molecule AFM to investigate the mechanical unfolding and folding of a plant type [2Fe-2S] ferredoxin from the cyanobacteria *Anabaena* (aFd).[28] AFd is a 98 residues long α/β protein that assumes a typical β-grasp fold, where a four-strand β-pleated sheet is packed against α-helices (Figure 1).

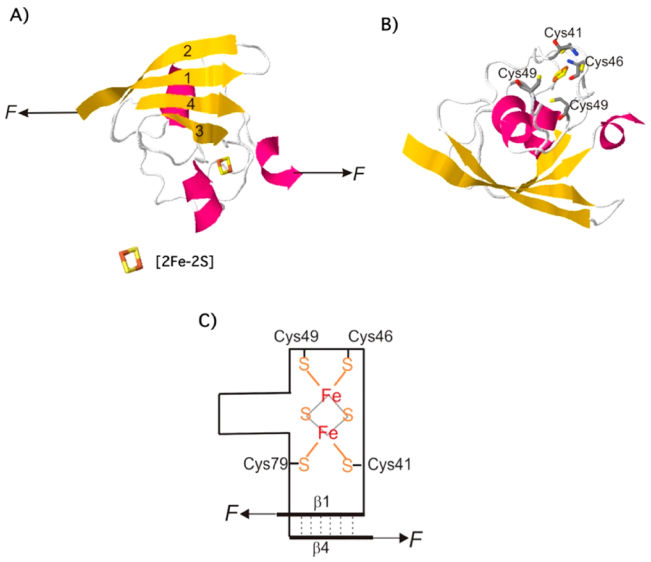

Figure 1. (A,B) The three-dimensional structure of oxidized ferredoxin from *Anabaena* (PDB code: 1fxa). The ferric ions are coordinated in a tetrahedral geometry by both inorganic sulfurs and sulfurs from four cysteine residues. The [2Fe-2S] cluster is highlighted in (A), where ferric ions are colored in red, and inorganic sulfurs in yellow. For simplicity, a schematic of aFd is shown in (C), where the thick lines indicate the two force bearing β-strands 1 and 4, and the dotted lines indicate backbone hydrogen bonds between the two strands.

The [2Fe-2S] center is located at the outer edge of the β-grasp fold, and two irons are coordinated in a tetrahedral fashion by both inorganic sulfurs and sulfurs from four cysteine residues (Cys41, 46, 49, and 79) in the −CxxxxCxxCx$_n$C− motif, which is common to plant type ferredoxins (Figure 1). The iron−sulfur center not only imparts functionality to ferredoxin, but may also stabilize it. In this study, we used the AFM to stretch the oxidized form of aFd from its N- and C-termini to investigate both its mechanical unfolding and refolding, as well as the role played by the iron−sulfur center in stabilizing aFd and mediating the folding of the native holo-aFd in vitro.

MATERIALS AND METHODS

Protein Engineering. The gene for ferredoxin from *Anabaena* (aFd) was custom synthesized (Genscript, U.S.), and designed to include 5′ *Bam*HI, and 3′ *Bgl*II and *Kpn*I restriction sites. The gene encoding the protein chimera Cys-aFd-GL15-Cys was constructed in the pQE80L vector (Qiagen, Valencia, CA) following standard molecular biology techniques (where the full amino acid sequence of Cys-aFd-GL15-Cys is shown in the Supporting Information). The protein chimera was overexpressed in the *Escherichia coli* strain DH5 α, and purified with Co^{2+} affinity chromatography using TALON resins (Clontech, Mountain View, CA). Figure S1 shows the SDS-PAGE photograph of purified Cys-aFd-GL15-Cys. Purified protein samples (~1.5 mg/mL) were stored in the elution buffer (50 mM Tris-HCl, 1 M NaCl, pH 7.4) at 4 °C until use. UV−vis spectroscopy was used to quantitatively determine the purity of aFd (NanoDrop ND-1000 UV−vis spectrometer; Thermo Scientific, Wilmington, DE). The ratio between the absorbance maxima at ~420 and ~280 nm (A_{420}/A_{280}) was used to calculate the percentage of holo-proteins, where a A_{420}/A_{280} ratio of 0.26 was considered to be ~100% pure holo-aFd-GL15 (Figure S2).[29]

The protein solution was concentrated to ~8 mg/mL using an Amicon Ultra-4 centrifugal filter unit equipped with a Ultracel-3 membrane (MILLIPORE, Billerica, MA). To construct the polyprotein (aFd-GL15)$_n$, we employed the thiol-maleimide coupling chemistry. Cys-aFd-GL15-Cys and BM(PEO)3 (1,8-bis-maleimido-(PEO)$_3$; Molecular Biosciences, Boulder, CO) were allowed to react with each other at 1:1 stoichiometry at room temperature, as previously reported.[17] The degree of polymerization (n) of the resultant (aFd-GL15)$_n$ ranges from 2 to 6 (Figure S1B).

Single-Molecule AFM Experiments. Single-molecule AFM experiments were carried out on a MFP3D AFM (Asylum Research, Santa Barbara, CA) as well as on a custom-made AFM, which was constructed as described previously.[30] Each Si_3N_4 cantilever (MLCT cantilevers; Bruker, Santa Barbara, CA) was calibrated in buffer before each experiment using the equipartition theorem, and a nominal spring constant is ~40 pN/nm. In a typical experiment, ~2 μL of cross-linked protein sample was deposited onto a clean glass coverslip covered with ~100 μL of buffer (100 mM Tris HCl, 1 M NaCl, pH 7.4). The sample was allowed to adsorb for about 20 min, after which ~4 mL of buffer was added. Constant-velocity AFM pulling experiments were performed at 400 nm/s, unless otherwise noted.

RESULTS

Mechanical Unfolding of Ferredoxin. To investigate the mechanical unfolding mechanism of aFd, we first constructed the Cys-aFd-GL15-Cys heterodimer, and used maleimide−thiol coupling chemistry to construct the polyprotein (aFd-GL15)$_n$ for single-molecule AFM experiments.[17] GL15 is a loop insertion variant of the small model protein GB1 in which a stretch of 15 flexible residues is inserted into the second loop of GB1.[31,32] The signatures of the mechanical unfolding of GL15 are a contour length increment (ΔL_c) of ~23 nm and a unfolding force of ~150 pN at a pulling speed of 400 nm/s, as detailed in our previous work.[32] The well-characterized GL15 domain serves both as a "fingerprint domain" for detecting single-molecule force spectrum for (aFd-GL15)$_n$, as well as an internal force caliper in the (aFd-GL15)$_n$ polyprotein.[32] Stretching the (aFd-GL15)$_n$ polyprotein allowed us to stretch aFd from its N- and C-termini. The [2Fe-2S] center is enclosed by the protein β-grasp fold structure of aFd, as shown in Figure 1C. The two force-bearing β-strands 1 and 4 of aFd constitute a mechanical clamp that provides resistance to the mechanical unfolding of aFd; thus, the [2Fe-2S] center will not likely experience any stretching force until this mechanical clamp has unraveled.

Stretching polyprotein (aFd-GL15)$_n$ leads to representative sawtooth-like force−extension curves shown in Figure 2A, in which each individual sawtooth peak corresponds to the force-induced unfolding of individual domains in the polyprotein chain. The last peak often arises from the detachment of the fully unfolded polypeptide chain, from either the glass substrate or the AFM tip. The unfolding force peaks of (aFd-GL15)$_n$ display three distinct populations that are colored differently in

DOI: 10.1021/jacs.6b11371
J. Am. Chem. Soc. 2017, 139, 1538−1544

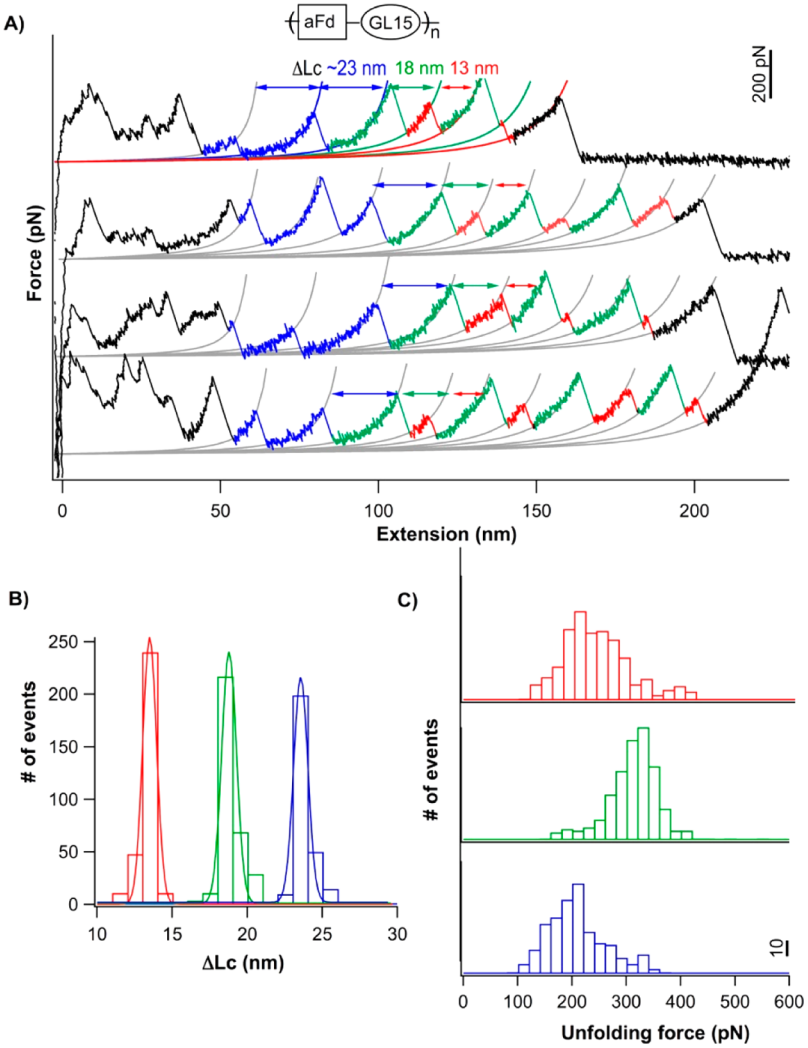

Figure 2. Mechanical unfolding of $(aFd\text{-}GL15)_n$ reveals a two-step unfolding mechanical of aFd. (A) Representative force−extension curves of $(aFd\text{-}GL15)_n$. Force−extension curves display three distinct ΔL_c's, signifying three different unfolding events. Mechanical unfolding events with ΔL_c of ∼23 nm (blue) correspond to the unfolding of the fingerprint domain GL15. Unfolding events with a ΔL_c of ∼18 nm (colored in green) and ∼13 nm (colored in red) relate to the unfolding of aFd. Thin solid lines are the WLC fits to the experimental data. A schematic of the polyprotein $(aFd\text{-}GL15)_n$ is shown in the top panel. (B) The histogram of ΔL_c from $(aFd\text{-}GL15)_n$ unfolding events displays three distinct peaks, which are centered around ∼13, ∼18, and ∼23 nm, respectively. Gaussian fits (solid lines) to the experimental data show average ΔL_c's of 12.8 ± 0.7 nm (avg ± std, n = 309), 18.2 ± 0.7 nm (n = 331), and 23.1 ± 0.8 nm (n = 284) for the three populations. (C) Unfolding force histogram of $(FdA\text{-}GL15)_n$ at a pulling speed of 400 nm/s. Unfolding of GL15 occurs at ∼200 pN, partial unfolding of aFd occurs at 311 ± 53 pN (n = 331), and mechanical rupture of the [2Fe-2S] cluster occurs at ∼240 ± 61 pN (n = 309).

the force−extension curves (Figure 2B), as signified by different contour length increments (ΔL_c) measured from the fits of the Worm-like Chain model of polymer elasticity[33] to the consecutive unfolding force events. One population of unfolding force events exhibited a ΔL_c of 23.1 ± 0.8 nm (blue events, Figure 2B), which is the characteristic feature of the mechanical unfolding of the fingerprint domain GL15. Thus, the other two populations of unfolding events can be readily assigned as the mechanical unfolding of aFd. WLC fits to the unfolding events reveal that these two populations of unfolding events have ΔL_c's of 18.2 ± 0.7 nm (colored in green) and 12.8 ± 0.7 nm (colored in red), respectively. It is interesting that these two unfolding events are always paired, where the event in green occurs first, followed by the event in red. Moreover, these two unfolding events display a reverse mechanical unfolding hierarchy,[34] where the mechanically more stable event (green) occurs prior to the mechanically weaker one (in red). This strongly indicates that these two unfolding events correspond to the stepwise unfolding of a single aFd protein. aFd contains 98 residues, and the distance between its N- and C-termini is 3.1 nm. Thus, the complete mechanical unfolding of aFd will lead to a ΔL_c of ∼32 nm (98 aa*0.36 nm/aa − 3.1 nm), which closely agrees with the sum of ΔL_{c1} and ΔL_{c2} from the two unfolding events. This suggests that the mechanical unfolding of aFd follows a two-step mechanism, where ΔL_{c1} and ΔL_{c2} should reveal important structural information about the force-induced unfolding mechanism of aFd.

Our previous studies on rubredoxin showed that the mechanical rupture of ferric−thiolate bonds occurs at ∼230 pN; thus, the protein structure/sequence enclosed by the FeS_4 center will not experience the stretching force until the metal center has ruptured.[20] Ferric−thiolate bonds in the [2Fe-2S] metal center of aFd are similar to those in rubredoxin, and

DOI: 10.1021/jacs.6b11371
J. Am. Chem. Soc. 2017, 139, 1538−1544

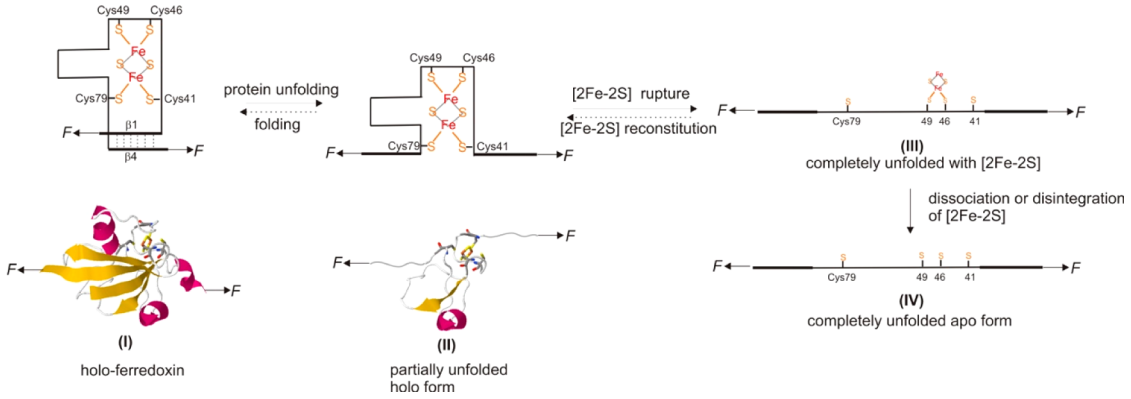

Figure 3. Schematic of the three-state unfolding process of holo-aFd under stretching force. The first step corresponds to the rupture of the mechanical clamp formed by the two terminal force-bearing β-strands 1 and 4. The protein structure encompassed by residues 41−79, which is sequestered by the [2Fe-2S] center until the rupture of [2Fe-2S] center, serves as an unfolding intermediate state. The second unfolding step corresponds to the forced rupture of ferric−thiolate bonds (likely between Fe(III)−Cys79 and other bonds), and subsequent unraveling of the remaining protein structure. The species (III) shown here is likely one of the few possible. Dotted arrows indicate a possible folding process, which reverses the unfolding process.

should thus be mechanically stable. Therefore, the [2Fe-2S] center will likely shield the sequence enclosed by the [2Fe-2S] center (residues 41−79) from the stretching force until the [2Fe-2S] metal center ruptures, giving rise to the two step unfolding behavior exhibited by aFd.

The unfolding of the aFd sequences outside the [2Fe-2S] center (residues 1−40 and 80−98) requires the rupture of the mechanical clamp formed by the two force-bearing β-strands 1 and 4. This would result in a ΔL_{c1} of 18.1 nm, according to (40 + 19) aa × 0.36 nm/aa − 3.1 nm, where 3.1 nm measures the distance between aFd's N- and C-termini. This predicted value agrees well with the experimentally measured ΔL_{c1}, suggesting that the first unfolding step (colored in green) arises from the unfolding of the aFd sequence that is directly exposed to the stretching force and outside of the [2Fe-2S] center. Accordingly, the second unfolding step should correspond to the rupture of the [2Fe-2S] center as well as the subsequent unfolding/extension of the protein sequence sequestered by this [2Fe-2S] center. Indeed, the rupture of the [2Fe-2S] center and protein structure unfolding should result in a ΔL_c of ∼12.8 nm according to 39 aa*0.36 nm/aa − 1.2 nm, where 1.2 nm measures the distance between Cys41 and Cys79. This agrees well with the experimentally observed ΔL_{c2}.

Therefore, the force-induced unfolding of aFd occurs in two steps: (1) partial unfolding of the aFd protein structure encompassing residues 1−40 and 80−98; and (2) rupture of the [2Fe-2S] metal center, and subsequent unfolding of the remaining protein structure (residues 41−79) (Figure 3). In this unfolding mechanism, the protein structure encompassing residues 41−79, which is sequestered by the [2Fe-2S] center and does not experience the stretching force until the rupture of the [2Fe-2S] center, serves as an unfolding intermediate state. It is of note that the [2Fe-2S] cluster is incorporated into aFd via the −CxxxxCxxCx$_n$C− motif. This motif is asymmetric due to the location of cysteines, where three cysteines (Cys41, 46, and 49) are clustered close together (as they are separated by four and two residues), while the fourth cysteine (Cys 79) is far apart (and is separated from Cys49 by 40 residues). Given the observed ΔL_{c2} of 12.8 nm, the rupture event of the [2Fe-2S] cluster is more likely to involve the ferric−thiolate bond between Fe(III) and Cys79, rather than result from the rupture of all three ferric−thiolate bonds between Fe(III) and Cys41, Cys46, and Cys49, while the ferric−thiolate bond between Fe(III) and Cys79 remains intact. However, mechanical rupture of ferric−thiolate bond Fe(III)-Cys(79) alone would give rise to a ΔL_{c2} of ∼11 nm (31 aa*0.36 nm/aa), which does not account for the observed ΔL_{c2}; thus, the rupture of additional ferric thiolate bond(s) likely also occurs. It remains to be established which of the remaining three ferric−thiolate bonds are ruptured during mechanical unfolding of aFd, and the order in which they do so.

Mechanical Rupture of the [2Fe-2S] Metal Center Occurs at ∼240 pN. The elucidation of the mechanical unfolding mechanism of aFd also allows us to unambiguously determine the mechanical stability of ferric thiolate bonds between ferric ions and cysteinyl sulfurs. The second unfolding/rupture step, which occurs at ∼240 pN, corresponds to the mechanical rupture of the [2Fe-2S] metal center (Figure 2C). Moreover, rupture forces of the [2Fe-2S] metal center show a broad distribution, which should reflect intrinsic features of the energy landscape governing the mechanical rupture of ferric−thiolate bonds.[35,36] According to the Bell−Evans model, the width of the rupture force distribution is inversely proportional to the distance from the bound state to the transition state (Δx_u),[35,36] and a broader distribution of the rupture forces suggests a shorter Δx_u. To quantify Δx_u during the mechanical unfolding of aFd and rupture of the [2Fe-2S] metal center, we measured the unfolding/rupture forces of aFd at different pulling speeds (Figure 4). As expected, with the increase of the pulling speed, the mechanical rupture force increases. Using well-established Monte Carlo simulation protocols,[35,37,38] we reproduced the sawtooth-like force−extension results of (aFd-GL15)$_n$. We found that the average unfolding forces and their pulling speed dependence for the mechanical rupture of the [2Fe-2S] center can be well-reproduced using a Δx_u of 0.13 nm and a spontaneous off rate at zero force (α_0) of 0.07 s^{-1} (Figure 4). A Δx_u of 0.13 nm for the metal center (which is roughly one-half of the ferric−thiolate bond length) is smaller than that typical for protein unfolding, but is considerably bigger than that for a disulfide bond (∼0.1−0.2 Å).[39] This result is similar to that of rubredoxin,[20] suggesting that the width of the potential well of the ferric−thiolate bonds is similar for both rubredoxin and aFd. Similarly, we estimated a Δx_u of 0.17 nm and α_0 of

DOI: 10.1021/jacs.6b11371
J. Am. Chem. Soc. 2017, 139, 1538−1544

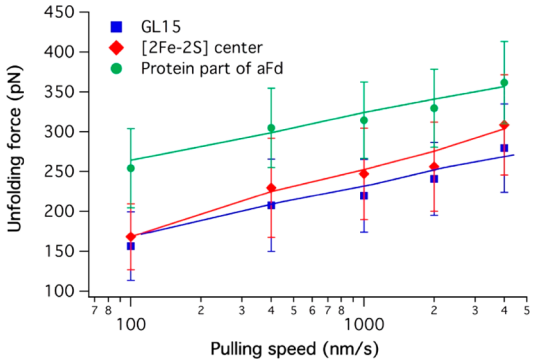

Figure 4. Pulling speed dependence of the unfolding/rupture forces for GL15 (in blue), the protein part of aFd (in green), and the [2Fe-2S] cluster (in red). Solid lines are Monte Carlo simulation results using a Δx_u of 0.13 ± 0.03 nm, and a spontaneous dissociation rate α_0 of 0.07 ± 0.01 s^{-1} for the cluster, Δx_u of 0.17 ± 0.03 nm and α_0 of 0.00051 ± 0.0001 s^{-1} for the protein part, and Δx_u of 0.17 ± 0.03 nm and α_0 of 0.025 ± 0.003 s^{-1} for GL15.

0.00051 s^{-1} for mechanical unfolding of the protein part of aFd, and a Δx_u of 0.17 nm and α_0 of 0.025 s^{-1} for the mechanical unfolding of the fingerprint domain GL15. It is interesting that aFd and GL15 both have a β-grasp fold structure,[29] where resistance to mechanical unfolding for both proteins likely corresponds to the simultaneous rupture of backbone hydrogen bonds between the two terminal force-bearing β-strands, giving rise to similar distances between the native and mechanical unfolding transition state for both proteins.

Refolding of Ferredoxin. One of the major difficulties in investigating the folding behavior of iron sulfur proteins using traditional ensemble experiments is the fact that iron sulfur protein unfolding is often irreversible. This is due to the disintegration of iron sulfur clusters upon unfolding, which are required for the metalloprotein to refold into its native holo-form.[40−43] As we demonstrated using rubredoxin, single-molecule force spectroscopy may offer a unique means of studying how metalloproteins fold following unfolding, including the disintegration of the iron sulfur cluster.[44] Here, we carried out single-molecule AFM refolding experiments to investigate whether aFd can refold after mechanical unfolding. In our AFM experiments, the protein was picked up from the glass substrate by the AFM tip through nonspecific interactions. Repeatedly stretching and relaxing the same $(aFd\text{-}GL5)_n$ molecule over many cycles was very challenging. We managed to obtain ∼10 molecules with each one lasting a limited number of stretching−relaxation cycles. Despite this difficulty, these preliminary results provided some invaluable insights, as shown in Figure 5, which highlights two such experiments. In the first molecule (Figure 5A), unfolding events for two GL15 (colored in blue) and two aFd domains are clearly visible (where the unfolding of the protein portion is shown in green, and the rupture of the metal center in red). In the subsequent force−extension curve (curve 2), we observed one GL15 unfolding event after the unfolded polypeptide was relaxed to zero force for 5 s, suggesting that only one of the two GL5 domains refolded. In addition, we observed an unfolding event with a ΔL_c of ∼13 nm, suggesting that only one [2Fe-2S] metal center was fully reconstituted between the two unfolded aFd domains; the protein part of this aFd domain did not refold. In the third force−extension curve for this molecule, we observed that one GL15 domain managed to refold (colored in blue). In

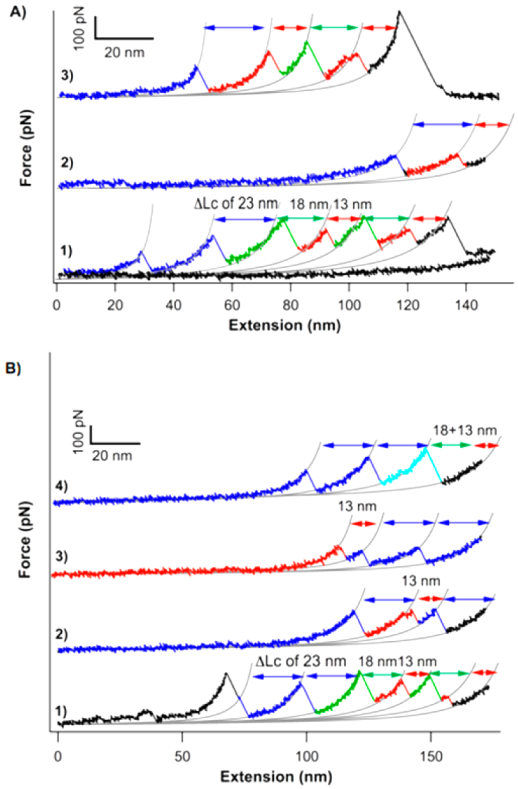

Figure 5. Reversible unfolding and refolding of aFd observed directly during repeated stretching and relaxation experiments from a single $(aFd\text{-}GL15)_n$ polyprotein. Two examples are shown in (A) and (B). Unfolding events (colored in green) show a ΔL_c of ∼18 nm, corresponding to the unfolding of the protein portion of aFd (which encompasses residues 1−40 and 80−98); unfolding events in red display a ΔL_c of ∼13 nm, corresponding to the mechanical rupture of the metal center in aFd. Unfolding events colored in blue correspond to an ΔL_c of 23 nm and the unfolding of GL15. The occurrence of holo-ferredoxin unfolding events during successive stretching−relaxation cycles indicates the successful reconstitution of the [2Fe-2S] cluster and the refolding of holo-ferredoxin.

addition, we observed one of the two aFd domains managed to refold completely to its native holo-form with the fully reconstituted [2Fe-2S] center, giving rise to the two-step unfolding appearance with a ΔL_{c1} of 18 and ΔL_{c2} of 13 nm. The second aFd domain only refolded partially: the rupture event of ΔL_c of 13 nm suggested that the [2Fe-2S] center in this aFd domain was successfully reconstituted, while the protein part did not refold. Figure 5B shows that a second $(aFd\text{-}GL5)_n$ molecule demonstrated similar behaviors. These results clearly indicate that the [2Fe-2S] metal center can reconstitute after ferric−thiolate bonds between cysteinyl sulfur and the [2Fe-2S] cluster are broken, and the unfolded aFd can refold into its native holo-form with a fully reconstituted [2Fe-2S] metal center. Moreover, these results imply that not all ferric-thiolate bonds rupture, and the [2Fe-2S] cluster was still coordinated to the unfolded aFd polypeptide chain via ferric−thiolate bond(s) after mechanical unfolding of aFd and rupture of the [2Fe-2S] metal center (Figure 3). It is notable that we observed one unfolding event (colored in cyan in curve 4, Figure 5B) with a ΔL_c of ∼31 nm during repeated stretching−relaxation experiments (Figure 5B), implying that the unfolded aFd successfully refolded to its apo-form. However, it is unknown whether the [2Fe-2S] cluster is still coordinated to

DOI: 10.1021/jacs.6b11371
J. Am. Chem. Soc. 2017, 139, 1538−1544

this apo-aFd domain, and thus unclear whether the [2Fe-2S] metal center can fully reconstitute after apo-aFd has folded.

DISCUSSION

By employing AFM-based single-molecule force spectroscopy and protein engineering techniques, we directly probed the mechanical unfolding and refolding of the small iron sulfur protein aFd, which contains a plant type [2Fe-2S] metal center. Our results reveal that the mechanical unfolding of AFd follows a two-step mechanism (Figure 3): (1) the partial unfolding of AFd, which leads to the unraveling of the protein structure outside of the [2Fe-2S] metal center and the exposure of this metal center to the solvent; and (2) rupture of the [2Fe-2S] metal center, and subsequent unraveling of the protein sequence enclosed by this [2Fe-2S] metal center. The mechanical stability of ferric−thiolate bonds in the [2Fe-2S] metal center is comparable to the bond strengths of ferric−thiolate bonds within rubredoxin.[20]

The folded structure of aFd belongs to the β-grasp fold family. Proteins in this family have been shown to exhibit significant mechanical stability, such as ubiquitin,[45] GB1,[46] protein L,[47] and SUMO proteins.[48] All of these proteins show typical all-or-none unfolding behaviors, with the major mechanical resistance residing in the mechanical force clamp formed by the two terminal force-bearing β-strands that are arranged into a shearing topology.[45,47,49] The first unfolding step of aFd is similar to two-state unfolding observed in other β-grasp proteins. The second unfolding step, which is absent in the mechanical unfolding of other β-grasp proteins, clearly demonstrates the protein structure stabilization effect provided by the [2Fe-2S] metal center. Moreover, we directly observed the refolding of the holo-ferredoxin (with a fully reconstituted [2Fe-2S] metal center) from the completely unfolded ferredoxin. This demonstrates the possibility that holo-ferredoxin could fold without the assistance of the ferredoxin biogenesis proteins in vitro, which may open new avenues to investigate both the unfolding/folding of ferredoxin and the chemical reactivity of the [2Fe-2S] center in vitro. However, many questions remain. During the folding process, we observed the partial refolding of ferredoxin with the fully reconstituted [2Fe-2S] metal center before the protein portion had fully refolded (as exhibited as the absence of unfolding events with a ΔL_c of 18 nm). It is not clear whether the reconstitution of the [2Fe-2S] metal center serves to nucleate folding of the protein portion, and whether it is thus an obligatory initial step for the in vitro refolding of holo-ferredoxin (Figure 3). Alternatively, is it possible that the protein part of ferredoxin could refold to provide a structural scaffold for the reconstitution of the [2Fe-2S] metal center. This could be the case for holo-rubredoxin folding, where apo-rubredoxin could provide the binding site for ferric ion. The folding of apo-ferredoxin could also prevent or slow the reconstitution of the [2Fe-2S] metal center in ferredoxin, such as that observed in the metalloprotein azurin.[5] Further in-depth work regarding the refolding mechanism of holo-ferredoxin in vitro is necessary to fully address these questions; such single-molecule experiments may also pave the way to directly investigating the working mechanism of various biogenesis proteins during the in vivo folding of ferredoxin.

ASSOCIATED CONTENT

Supporting Information

The Supporting Information is available free of charge on the ACS Publications website at DOI: 10.1021/jacs.6b11371.

Amino acid sequence of Cys-aFd-GL15-Cys; Coomassie blue stained sodium dodecyl sulfate polyacrylamide gel electrophoresis of aFd-GL15 and $(aFd\text{-}GL15)_n$, and UV−vis spectrum of $(aFd\text{-}GL15)_n$ (PDF)

AUTHOR INFORMATION

Corresponding Author

*hongbin@chem.ubc.ca

ORCID

Hongbin Li: 0000-0001-7813-1332

Notes

The authors declare no competing financial interest.

ACKNOWLEDGMENTS

We thank Dr. Peng Zheng, Devin Li, and Kailin Zhou for their preliminary experiments and helpful discussion. This work was supported by the Natural Sciences and Engineering Research Council of Canada, the Canada Foundation for Innovation, the Canada Research Chairs Program, and the National Natural Sciences Foundation of China. Ha.L. acknowledges a fellowship from the China Scholarship Council.

REFERENCES

(1) Holm, R. H.; Kennepohl, P.; Solomon, E. I. *Chem. Rev.* **1996**, *96*, 2239−2314.
(2) Gray, H. B. *Proc. Natl. Acad. Sci. U. S. A.* **2003**, *100*, 3563−3568.
(3) Johnson, D. C.; Dean, D. R.; Smith, A. D.; Johnson, M. K. *Annu. Rev. Biochem.* **2005**, *74*, 247−281.
(4) Waldron, K. J.; Rutherford, J. C.; Ford, D.; Robinson, N. J. *Nature* **2009**, *460*, 823−830.
(5) Wittung-Stafshede, P. *Acc. Chem. Res.* **2002**, *35*, 201−208.
(6) Bushmarina, N. A.; Blanchet, C.; Vernier, G.; Forge, V. *J. Phys. IV* **2005**, *130*, 209−228.
(7) Dudev, T.; Lim, C. *Annu. Rev. Biophys.* **2008**, *37*, 97−116.
(8) Loh, S. N. *Metallomics* **2010**, *2*, 442−449.
(9) Rakhit, R.; Chakrabartty, A. *Biochim. Biophys. Acta, Mol. Basis Dis.* **2006**, *1762*, 1025−1037.
(10) Bertini, I.; Cowan, J. A.; Luchinat, C.; Natarajan, K.; Piccioli, M. *Biochemistry* **1997**, *36*, 9332−9339.
(11) Crampton, N.; Brockwell, D. J. *Curr. Opin. Struct. Biol.* **2010**, *20*, 508−517.
(12) Hoffmann, T.; Dougan, L. *Chem. Soc. Rev.* **2012**, *41*, 4781−4796.
(13) Javadi, Y.; Fernandez, J. M.; Perez-Jimenez, R. *Physiology* **2013**, *28*, 9−17.
(14) Puchner, E. M.; Gaub, H. E. *Curr. Opin. Struct. Biol.* **2009**, *19*, 605−614.
(15) Marszalek, P. E.; Dufrene, Y. F. *Chem. Soc. Rev.* **2012**, *41*, 3523−3534.
(16) Zocher, M.; Bippes, C. A.; Zhang, C.; Muller, D. J. *Chem. Soc. Rev.* **2013**, *42*, 7801−7815.
(17) Zheng, P.; Cao, Y.; Li, H. *Langmuir* **2011**, *27*, 5713−5718.
(18) Zheng, P.; Li, H. *Biophys. J.* **2011**, *101*, 1467−1473.
(19) Zheng, P.; Arantes, G. M.; Field, M. J.; Li, H. *Nat. Commun.* **2015**, *6*.
(20) Zheng, P.; Li, H. *J. Am. Chem. Soc.* **2011**, *133*, 6791−6798.
(21) Kudera, M.; Eschbaumer, C.; Gaub, H. E.; Schubert, U. S. *Adv. Funct. Mater.* **2003**, *13*, 615−620.
(22) Wei, W.; Sun, Y.; Zhu, M.; Liu, X.; Sun, P.; Wang, F.; Gui, Q.; Meng, W.; Cao, Y.; Zhao, J. *J. Am. Chem. Soc.* **2015**, *137*, 15358−15361.

DOI: 10.1021/jacs.6b11371
J. Am. Chem. Soc. 2017, 139, 1538−1544

(23) Beedle, A. E.; Lezamiz, A.; Stirnemann, G.; Garcia-Manyes, S. *Nat. Commun.* **2015**, *6*, 7894.
(24) Perales-Calvo, J.; Lezamiz, A.; Garcia-Manyes, S. *J. Phys. Chem. Lett.* **2015**, *6*, 3335−3340.
(25) Leal, S. S.; Gomes, C. M. In *Protein Folding and Metal Ions: Mechanisms, Biology and Disease*; Cláudio, M., Gomes, P. W.-S., Eds.; CRC Press: Boca Raton, FL, 2010; pp 81−94.
(26) Harayama, S.; Polissi, A.; Rekik, M. *FEBS Lett.* **1991**, *285*, 85−88.
(27) Lill, R. *Nature* **2009**, *460*, 831−838.
(28) Rypniewski, W. R.; Breiter, D. R.; Benning, M. M.; Wesenberg, G.; Oh, B. H.; Markley, J. L.; Rayment, I.; Holden, H. M. *Biochemistry* **1991**, *30*, 4126−4131.
(29) Fukuyama, K. *Photosynth. Res.* **2004**, *81*, 289−301.
(30) Fernandez, J. M.; Li, H. *Science* **2004**, *303*, 1674−1678.
(31) Li, H.; Wang, H. C.; Cao, Y.; Sharma, D.; Wang, M. *J. Mol. Biol.* **2008**, *379*, 871−880.
(32) Wang, Y.; Hu, X.; Bu, T.; Hu, C.; Hu, X.; Li, H. *Langmuir* **2014**, *30*, 2761−2767.
(33) Marko, J. F.; Siggia, E. D. *Macromolecules* **1995**, *28*, 8759−8770.
(34) Peng, Q.; Li, H. B. *J. Am. Chem. Soc.* **2009**, *131*, 14050−14056.
(35) Evans, E. *Annu. Rev. Biophys. Biomol. Struct.* **2001**, *30*, 105−128.
(36) Bell, G. I. *Science* **1978**, *200*, 618−627.
(37) Rief, M.; Fernandez, J. M.; Gaub, H. E. *Phys. Rev. Lett.* **1998**, *81*, 4764−4767.
(38) Oberhauser, A. F.; Marszalek, P. E.; Erickson, H. P.; Fernandez, J. M. *Nature* **1998**, *393*, 181−185.
(39) Garcia-Manyes, S.; Liang, J.; Szoszkiewicz, R.; Kuo, T. L.; Fernandez, J. M. *Nat. Chem.* **2009**, *1*, 236−242.
(40) Morleo, A.; Bonomi, F.; Iametti, S.; Huang, V. W.; Kurtz, D. M., Jr. *Biochemistry* **2010**, *49*, 6627−6634.
(41) Prakash, S.; Sundd, M.; Guptasarma, P. *PLoS One* **2014**, *9*, e89703.
(42) Moczygemba, C.; Guidry, J.; Jones, K. L.; Gomes, C. M.; Teixeira, M.; Wittung-Stafshede, P. *Protein Sci.* **2001**, *10*, 1539−1548.
(43) Wittung-Stafshede, P.; Gomes, C. M.; Teixeira, M. *J. Inorg. Biochem.* **2000**, *78*, 35−41.
(44) Zheng, P.; Wang, Y.; Li, H. *Angew. Chem., Int. Ed.* **2014**, *53*, 14060−14063.
(45) Carrion-Vazquez, M.; Li, H.; Lu, H.; Marszalek, P. E.; Oberhauser, A. F.; Fernandez, J. M. *Nat. Struct. Biol.* **2003**, *10*, 738−743.
(46) Cao, Y.; Li, H. *Nat. Mater.* **2007**, *6*, 109−114.
(47) Brockwell, D. J.; Beddard, G. S.; Paci, E.; West, D. K.; Olmsted, P. D.; Smith, D. A.; Radford, S. E. *Biophys. J.* **2005**, *89*, 506−519.
(48) Kotamarthi, H. C.; Sharma, R.; Ainavarapu, R. K. *Biophys. J.* **2013**, *104*, 2273−2281.
(49) Glyakina, A. V.; Balabaev, N. K.; Galzitskaya, O. V. *J. Chem. Phys.* **2009**, *131*, 045102.

DOI: 10.1021/jacs.6b11371
J. Am. Chem. Soc. 2017, 139, 1538−1544